



Study of the Nonlinear Mode-tide Coupling of Coalescing Binary Neutron Stars in Relativistic Formalism

Abhishek Das, Fatemeh Hossein-Nouri, Sukanta
Bose, Matt Duez

The Brief History of Mode-tide Coupling Instabilities in NSNS Systems

- **Weinberg et al. (ApJ, 769, 121, 2015)** proposed p -g tidal instability, in which the tidal bulge excites a low-frequency g-mode and a high frequency p-mode, can extract orbital energy, and cause a phase shift in the GW signal from the early inspiral phase, observable by gravitational wave detectors.
- **Venumadhav et al. (ApJ, 781, 23, 2015)** showed in second order perturbation, assuming a *static tide*, near-exact *cancellation* occurs between the three and four-mode couplings, which reduced the growth rate and implied that the instability cannot affect the inspiral significantly.
- **Weinberg (ApJ, 819, 109, 2016)** relaxed simplifying assumptions, allowing the stars become compressible under the influence of *non-static linear tides*. As a result, the near-exact cancellation is undone, and the instability becomes important once again.
- **Zhou & Zhang (ApJ, 849,114, 2017)** computed mode-tide coupling strength (MTCS) for TOV models using six different equations of state for both static (time-independent) and non-static tides.

Zhou & Zhang's MTCS studies (2017)

Mode-tide coupling strength (MTCS) computed applying the same formalism introduced in Weinberg's and Venumadhav's works using perturbation theory, to study the effects of EOS on the MTCS.

- 1) Confirm the near-exact cancellation happens between three and four mode couplings for static tides.
- 2) Stronger mode-tide coupling for non-static tides, trigger the instability in late inspiral phase.

TABLE 3

THE MTCS EVALUATED WITH THE $l_g = 4$, $n = 32$ EXAMPLE G-MODES AT $A = 95$ KM (NO RESONANCE OCCURS AT THIS BINARY SEPARATION), TOGETHER WITH THE INSTABILITY THRESHOLD AND THE DURATION OF THE INSTABILITY GROWTH WINDOW.

EOS	f_g (Hz)	MTCS ($A = 95$ km)		Instability Threshold (km)	t_{mg} (ms)
		Static tide	Non-static tide		
SLy4	2.71	1.75×10^{-3}	2.01	144	1583
Shen	27.7	1.60×10^{-4}	1.23×10^{-2}	57.0	35.4
APR1	23.3	4.53×10^{-5}	9.71×10^{-2}	41.2	10.1
APR2	23.7	2.99×10^{-5}	5.27×10^{-2}	46.8	16.9
APR3	15.9	5.58×10^{-5}	1.91×10^{-2}	58.9	42.8
APR4	18.8	3.95×10^{-5}	4.10×10^{-2}	54.4	30.7

MTCS equations:

g-mode frequency shift resulting from tidal perturbations. Keeping the leading order, we have:

$$\frac{\omega_-^2}{\omega_g^2} = 1 - \underbrace{\epsilon |U_{gg} + 2\kappa_{\chi gg}|}_{\text{MTCS}} + \mathcal{O}(\epsilon^2)$$

- $\kappa_{\chi gg}$: coupling coefficient between g-mode and the tide.
- U_{gg} : defined as $-\frac{1}{E_0} \int d^3x \rho \xi_a \cdot (\xi_b \cdot \nabla) \nabla U$
- ϵ : tidal strength defined as R^3/A^3
- ω_- : is the perturbed g-mode frequency
- ω_0 : characteristic frequency $\sqrt{GM/R^3}$

Static tide:

The tidal field (ϵU) is time-independent:

$$U \approx -\omega_0^2 r^2 P_2(\cos\theta)$$

Non-static tide:

The tidal field (ϵU) is time-dependent:

$$U_{\text{full}} \approx -\omega_0^2 r^2 \sum_{m=-2}^2 W_{2m} Y_{2m}(\theta, \phi) e^{-im\Omega t}$$

The dimensionless MTCS value determines how much the g-mode frequency is shifted due to the coupling with the tide.

$$\frac{\omega_-^2}{\omega_g^2} \approx 1 - \epsilon |MTCS|$$

When $MTCS > 1$, the perturbed frequency ω_- becomes imaginary and exponentially drives the mode to large amplitudes.

New stuff added to our work:

Zhou & Zhang (2017):

- ADIPLS package used to derive eigen–modes of neutron stars, which means Newtonian adiabatic oscillation equations for a relativistic star!!!
- Some hydro variables are defined in Newtonian way, which are not consistent for a relativistic system.
- The Cowling approximation (neglecting the perturbation to gravitational potential from g-mode) was used to compute MTCS, but has not been applied to the rest of the computations, i.e. eigenmodes.

Our work:

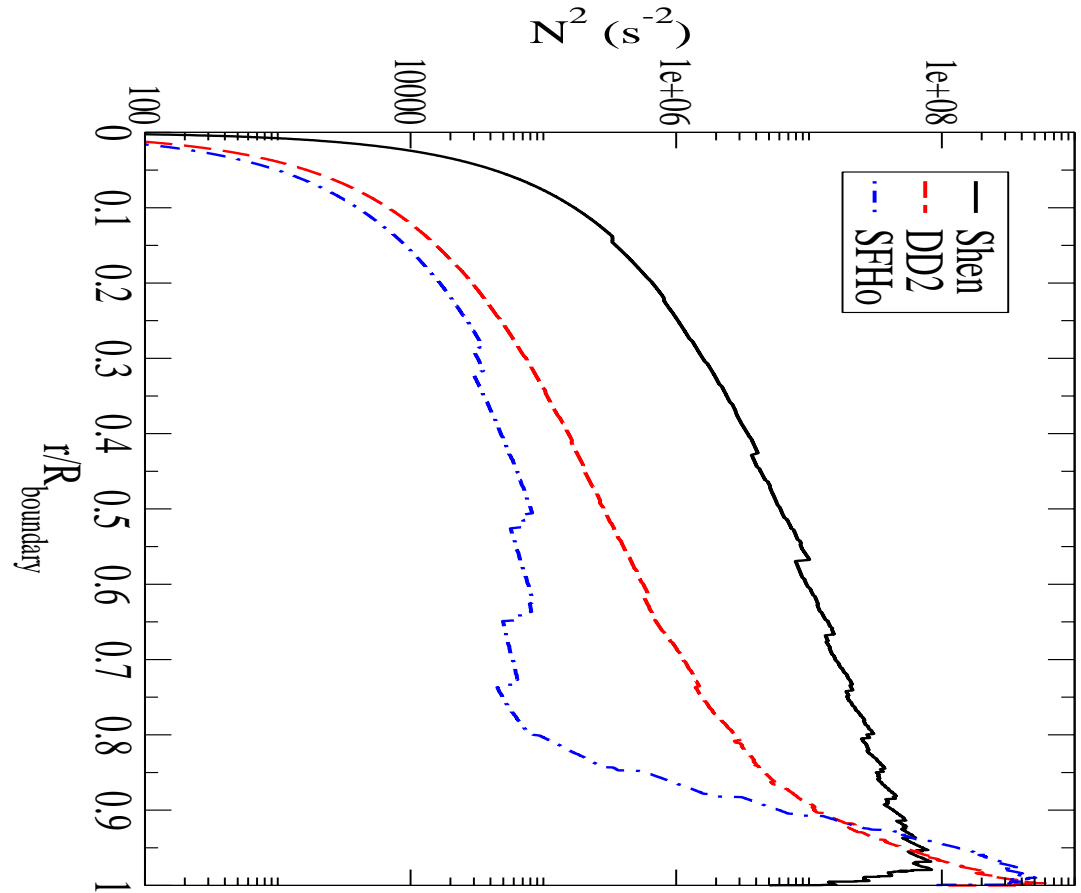
- We add relativistic corrections to ZZ’s MTCS computation by:
- 1- Developing our own code to compute relativistic eigenmodes in the Cowling approximation.
- 2- Using the relativistic definition of hydro variables for consistency.
- 3- Using more updated relativistic nuclear equations of state (such as SFHo, DD2)
- For a better comparison and study how significant these relativistic components are, we compute MTCS in pure Newtonian formalism as well (the background star is still relativistic).

Equations of State

- The central density adjusted to have equal mass for all the TOV models, $M = 1.4 M_{\odot}$

EOS	SFHo	DD2	Shen
R (km)	11.25	13.22	14.53

- We consider only core g-modes by resetting the Brunt-Vaisala frequency to zero in the crust region.
- Crust-core boundary is determined by choosing the position where Y_e hits its minimum.
- The neutron stars in the binary system are identical (equal mass and radius)



Brunt-Vaisala frequency for different EOS

Results: Static Tide

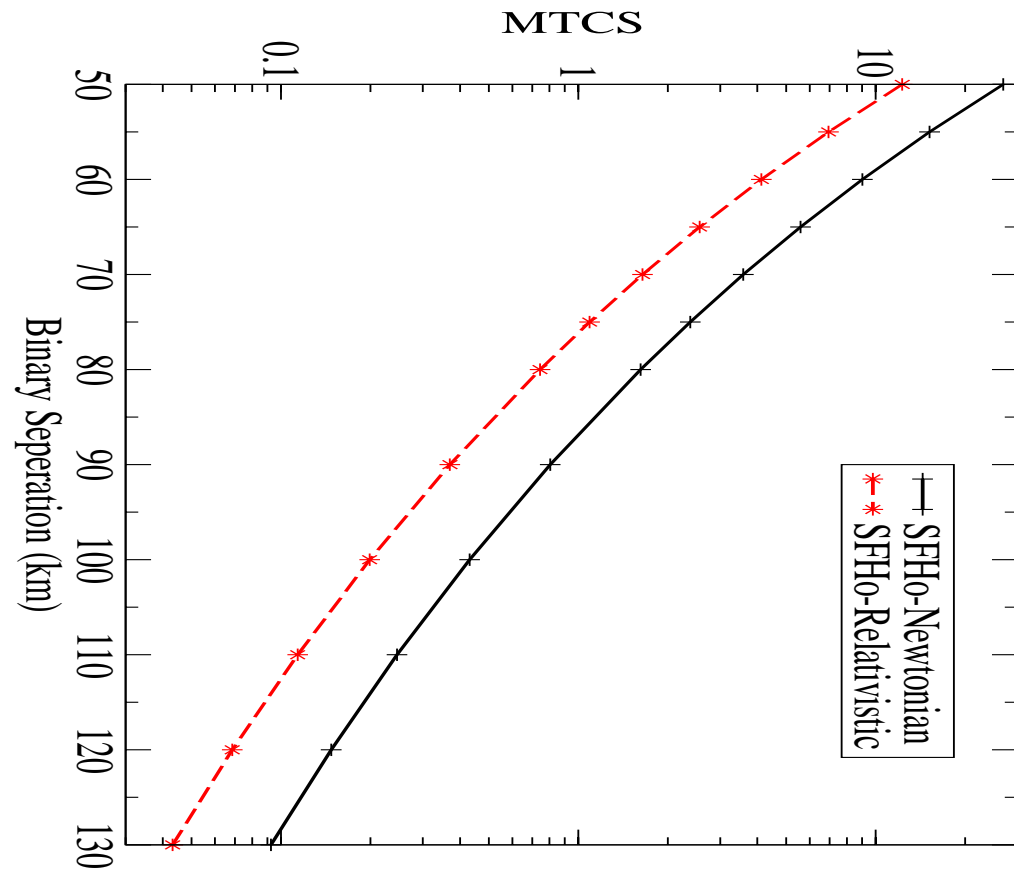
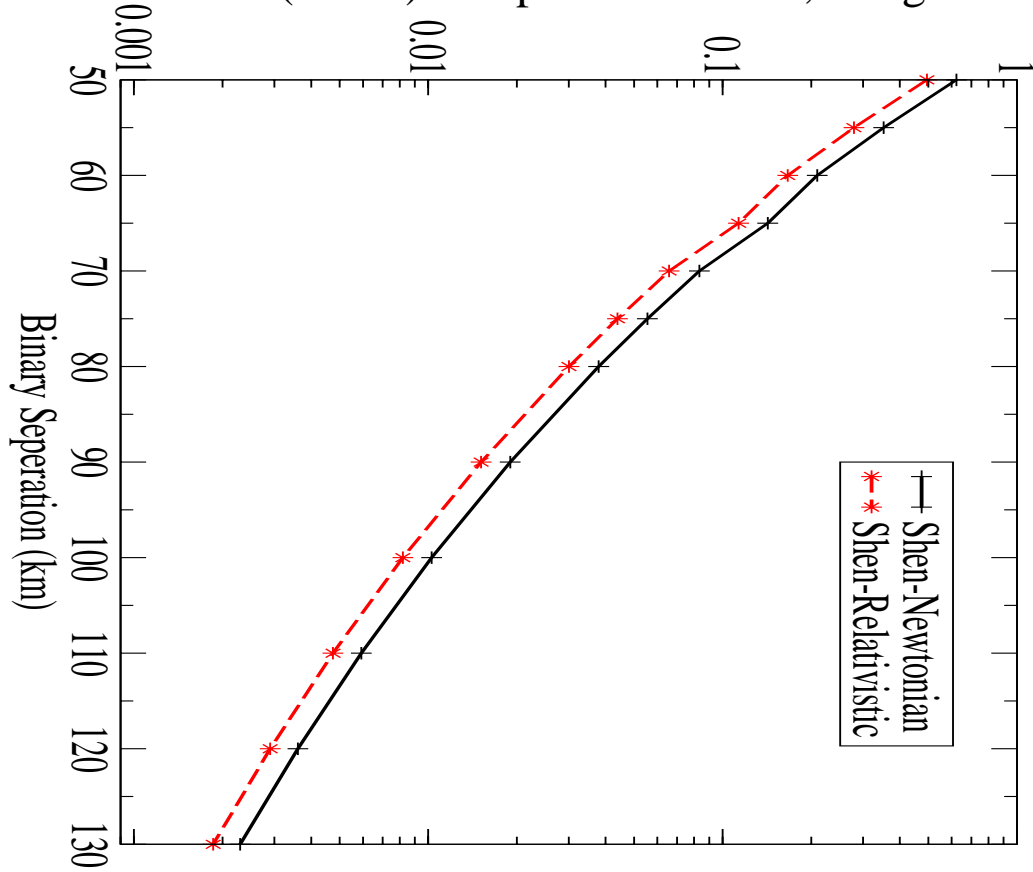
MTCS computed for static tide for two binary separations, $A=100$ km, and $A=2R$, for g-mode, $n=32$, $l_g=4$

- The relativistic corrections change the MTCS only by a few percent.
- MTCS is still too small to trigger the instability during inspiral.

EOS	MTCS (Newtonian) ($A = 2R$)	MTCS (Relativistic) ($A = 2R$)	MTCS (Newtonian) ($A = 100$ km)	MTCS (Relativistic) ($A = 100$ km)
Shen	0.2466	0.2621	0.000258	0.000282
DD2	0.2955	0.3901	0.000349	0.000418
SFHo	1.19	1.07	0.000312	0.000335

Results: Non-static (Time-dependent) Tide

Newtonian and relativistic MTCS for non-static tide verses binary separation for a stiff EOS (Shen), and for a soft EOS (SFHo) computed for $n=32, l=4$ g-mode.



Results: Non-static tide and Instability Threshold

The Newtonian and relativistic MTCS evaluated for g-mode $n=32$, $l=4$, for non-static tides with binary separation $A=95$ km. The instability threshold happens at the binary separation where MTCS exceeds 1.

EOS	$f_{g(N)} \text{ (Hz)}$	$f_{g(R)} \text{ (Hz)}$	$\text{MTCS}_{(N)}$	$\text{MTCS}_{(R)}$	$\text{Threshold}_{(N)} \text{ (km)}$	$\text{Threshold}_{(R)} \text{ (km)}$
Shen	36.06	27.46	0.01384	0.01103	48.3*	47.2*
DD2	14.15	10.91	0.01866	0.01212	54*	52*
SFHo	11.45	8.91	0.5837	0.2688	86.8	75.9

* These values are estimated based on other data points, and not very accurate.

Conclusions (so far)

- The relativistic corrections have the major effect in the softer equation of state, decrease the MTCS for non-static tide by more than 50% for SFHo.
- The relativistic corrections could only shift the MTCS for static tide by a few percent, the magnitude of the MTCS is still too low to cause any instability.
- For non-static tide, the relativistic corrections make the MTCS smaller over a wide range of binary separations, this would shift the instability threshold to smaller binary separations (late inspiral phase).
- EOS with lower Brunt-Vaisala frequency has stronger MTCS.

Future Work

- Consider crust g-modes (we should probably add a suitable crust treatment first, i.e. adding a shear stress term, etc)
- Compute MTCS for Higher order g-modes. Based on what proposed by Weinberg et al. (2015), the coupling is stronger for higher modes, which can trigger the instability in earlier time of the inspiral phase.
- Consider other EOS, to study the effects of stiffness on the MTCS.

MTCS main equations:

Static tide:

Eq(33) from Zhou
& Zhang (2017)

$$\begin{aligned}
 \text{MTCS} &\equiv \epsilon^2 |2\kappa_{gg\sigma} + V_{gg}| \\
 &\approx -\frac{1}{E_0} \int dr \rho g_r^2 c^2 \left\{ \left[\Gamma_1 + 1 + \left(\frac{\partial \ln \Gamma_1}{\partial \ln \rho} \right)_s \right] \right. \\
 &\quad \times \left(r \frac{dX}{dr} + 3X \right) \frac{r^2 \mathfrak{g}_1^2}{c_{s1}^2} - 4X \frac{r^2 \mathfrak{g}_1^2}{c_{s1}^2} \\
 &\quad - 2r^2 \left(r \Lambda_g^2 \frac{\omega_g^2}{c^2} \frac{g_h^2}{g_r^2} + 2\mathfrak{g}_1 \right) \frac{dX}{dr} - \mathfrak{g}_1 r^3 \frac{d^2 X}{dr^2} \\
 &\quad \times \left[-r^2 \mathfrak{g}_1 \frac{dX}{dr} - r \mathfrak{g}_1 X + r^2 X \frac{d\mathfrak{g}_1}{dr} \right. \\
 &\quad \left. - \frac{(6-n)(3-n)r^3}{10A^6 \mathfrak{g}_1} \left(\frac{GM}{c^2} \right)^2 \right] \\
 &\quad \left. \times \left(\frac{2r\mathfrak{g}_1}{c_{s1}^2} + \frac{d \ln \rho}{d \ln r} \right) \right\},
 \end{aligned}$$

Non-static tide:

Eq.(43-45) from Zhou
& Zhang (2017)

$$\begin{aligned}
 \text{MTCS} &\equiv \epsilon |U_{gg} + 2\kappa_{\chi^{(1)}gg,I} + 2\kappa_{\chi^{(1)}gg,H}| \\
 &\approx \epsilon \left| \frac{1}{E_0} \int dr \{ T \rho r^2 c_s^2 [\Gamma_1 + 1 \right. \\
 &\quad + \left. \left(\frac{\partial \ln \Gamma_1}{\partial \ln \rho} \right)_s \right] \nabla \cdot \chi^{(1)} (\nabla \cdot \mathbf{g})_r^2 \\
 &\quad + T \rho c_s^2 [2 \nabla \cdot \chi^{(1)} (\nabla \cdot \mathbf{g})_r (g_h \Lambda_g^2 - 4g_r) \\
 &\quad + (\nabla \cdot \mathbf{g})_r^2 (\chi_h^{(1)} \Lambda_x^2 - 4\chi_r^{(1)})] \\
 &\quad + T \rho \frac{d \ln \rho}{d \ln r} \left(4\mathfrak{g} + r \frac{d\mathfrak{g}}{dr} \right) \chi_r^{(1)} g_r^2 \\
 &\quad + T \rho r \left(4\mathfrak{g} + r \frac{d\mathfrak{g}}{dr} \right) [\nabla \cdot \chi^{(1)} g_r^2 \\
 &\quad \left. + 2(\nabla \cdot \mathbf{g})_r g_r \chi_r^{(1)} \right] \quad (43)
 \end{aligned}$$

$$\begin{aligned}
 &- \rho r \chi_h^{(1)} g_h g_h (\omega_x^2 G_x + \omega_g^2 G_g + \omega_g^2 G_g) \\
 &- \rho r \chi_r^{(1)} g_h g_h [(\omega_x^2 - 3\omega_g^2 - 3\omega_x^2) F_x - 2(\omega_g^2 F_g + \omega_g^2 F_g)] \\
 &- \rho r \chi_h^{(1)} g_r g_h [(\omega_g^2 - 3\omega_x^2 - 3\omega_x^2) F_g - 2(\omega_g^2 F_g + \omega_x^2 F_x)] \\
 &- \rho r \chi_h^{(1)} g_r g_h [(\omega_g^2 - 3\omega_x^2 - 3\omega_g^2) F_g - 2(\omega_x^2 F_x + \omega_g^2 F_g)] \\
 &+ \rho r \chi_h^{(1)} g_r g_r (\omega_g^2 F_g + \omega_g^2 F_g - 6\omega_x^2 T) \\
 &+ \rho r \chi_r^{(1)} g_r g_h (\omega_g^2 F_g + \omega_x^2 F_x - 6\omega_g^2 T) \\
 &+ \rho r \chi_r^{(1)} g_r g_h (\omega_x^2 F_x + \omega_g^2 F_g - 6\omega_g^2 T) \quad (44)
 \end{aligned}$$

$$- W_{lm} \frac{T(l+2)}{M \mathcal{R}^l} \int dr \rho r^l \left[\frac{\partial \ln \rho}{\partial \ln r} g_r^2 + 2r g_r (\nabla \cdot \mathbf{g})_r \right] \Big|, \quad (45)$$